Drying Technology

An International Journal

ISSN: (Print) (Online) Journal homepage: https://www.tandfonline.com/loi/ldrt20

Experimental study of paper drying with direct-contact ultrasound mechanism

Zahra Noori O'Connor, Jamal S. Yagoobi & Burt S. Tilley

To cite this article: Zahra Noori O'Connor, Jamal S. Yagoobi & Burt S. Tilley (2022): Experimental study of paper drying with direct-contact ultrasound mechanism, Drying Technology, DOI: 10.1080/07373937.2022.2150635

To link to this article: https://doi.org/10.1080/07373937.2022.2150635

DRYING TECHNOLOGY
https://doi.org/10.1080/07373937.2022.2150635

Experimental study of paper drying with direct-contact ultrasound mechanism

Zahra Noori O'Connor[a,b], Jamal S. Yagoobi[a,b], and Burt S. Tilley[c]

[a]Center for Advanced Research in Drying, Worcester Polytechnic Institute, Worcester, MA, USA; [b]Multi-Scale Heat Transfer Laboratory, Mechanical and Materials Engineering Department, – Worcester Polytechnic Institute, Worcester, MA, USA; [c]Center for Industrial Mathematics and Statistics, Department of Mathematical Sciences, Worcester Polytechnic Institute, Worcester, MA, USA

ABSTRACT

A systematic-study is conducted using an innovative technology for paper drying by applying ultrasound mechanism. The advantages include greater energy efficiency, lower drying time and temperature, improvement of the product quality, and it is considered a green technology. The effects of initial moisture content, thickness, and refining condition are studied for different types of pulps (hardwood and softwood) using 2^3 factorial design of experiments. Analysis of Variance show that in the range of the studied parameters, thickness has the maximum effect on ultrasonic drying time followed by the initial moisture content. In addition, using a linear regression model, a relationships for the total time of drying is provided. The results confirmed that ultrasonic drying is more efficient at higher moisture content and higher thickness of the sample. These results are related to the structural characteristic of the samples such as porosity, pore distribution, and surface roughness.

ARTICLE HISTORY
Received 6 February 2022
Revised 26 September 2022
Accepted 17 November 2022

KEYWORDS
Drying of paper;
ultrasonic drying;
quality measurements;
energy analysis

1. Introduction

In an energy-hungry industry such as paper-making, the main challenge is to improve the energy efficiency of the process. As one of the most important components in paper-making, the dryer section has a great impact on the overall energy consumption. According to Mujumdar,[1] although only 1% of original water is removed in the dryer section, it is still the most expensive and energy intensive unit in paper-making process. The dryer section costs 40% of total capital cost and consumes more than 60% of the total energy used in the paper machine.[2] Thus, any improvement in paper drying process may have a significant impact on the energy consumption and carbon footprint at the global level. Besides improvements to the current drying processes, developing new drying technologies is necessary to decrease the energy consumption. One of the most recently developed technologies for drying purposes that has attracted attention in the last few decades is the ultrasound assisted drying (UAD). Many studies have been devoted to developing ultrasonic drying in different applications including food conservation industries[3–9] and fabric drying.[10–12] UAD has widely shown effectiveness on enhancing the drying processes including freeze-drying, hot air drying, vacuum drying, and fluidized bed drying. This mechanism has potentials in decreasing the drying time, enhancing the energy efficiency, and preserving the quality of the dried product.[13] Specifically, in the beginning of the current century, researchers have become more interested in investigating this drying technology.[14–16]

Ultrasound is defined as the acoustic waves with the frequencies higher than the upper limit of the human hearing range, usually around 16–20 kHz.[17] Vibrations in the range of ultrasonic wave frequencies have the excellent characteristic of transporting the energy to a great distance in the liquid phase without significant dissipation. Ultrasonic waves have chemical and mechanical effects[18] and experiments have shown that ultrasound vibration represents the effects such as agitation, acoustic streaming, thermal effects, cavitation, and atomization. The effects of ultrasound depend on many factors, including specific drying condition, the nature of the material to be dried and the ultrasonic equipment; and the mechanism may vary significantly.[13] For instance, Peng et al.[10] reported that at high moisture contents, ultrasound induces acoustic nebulization and below a certain initial moisture content, ultrasound tends to just generate heat. There are two approaches for applying

CONTACT Zahra Noori O'Connor; znoori@wpi.edu Center for Advanced Research in Drying, Worcester Polytechnic Institute, Worcester, MA, USA.

ultrasound mechanism to a medium: non-contact and direct-contact. The original application of direct-contact ultrasound at high-frequency was introduced by researchers in the Oak Ridge National Laboratory (ORNL)[10,19] to assist fabric and clothes drying.

The unique advantage of direct-contact UAD, also known as high-frequency ultrasound, is inducing atomization. There are two proposed mechanisms of ultrasonic atomization: capillary theory and cavitation theory.[10,20] According to the capillary theory, ultrasound generates capillary waves at the liquid-vapor interface upon the excitation of a liquid droplet. At sufficiently high oscillation intensities, the interface becomes unstable and as a result the liquid ruptures to form fine mist. The hypothesis in cavitation theory is that the atomization happens through the hydraulic shocks generated by the implosion of cavitation bubbles, especially near the interface of liquid and gas. Atomization helps in mechanically removing of the moisture content in the form of mist, separating water from the porous material without thermal evaporation and thus, largely saving time and decreasing the energy consumption. Momen et al[19] reported significant impacts of the atomization on reducing drying time from hours to seconds and reducing energy consumption of the unit by an order of magnitude. Atomization helps in enabling high energy transfer efficiency from the transducer to the materials. On the other hand, the disadvantages of acoustic atomization are inducing thermal effects and requiring the presence of an important amount of bulk liquid, which limit the application of this drying technology.[13] More information about UAD can be found in the review paper by Zhang and Abatzoglou.[13]

To the best of the authors' knowledge, ultrasound assisted drying of paper products has not been investigated fundamentally. This paper is devoted to experimentally understand the effects of controlling parameters on direct-contact ultrasonic drying of paper samples. The independent variables considered in this study are the initial dry-basis moisture content (DBMC), final thickness of the sample, and refining condition of the pulp (unrefined vs refined). The methodology used is the 2^3 factorial design of experiments to be able to investigate the main and interactive effects among the independent variables on paper drying characteristics. In addition, the roughness, whiteness index, and tensile strength of the ultrasonically dried samples are studied. It is important to mention that drying of paper is a continuous and not a batch process. Thus, the application of ultrasound mechanism with direct-contact transducers in paper drying is not practical. Nevertheless, this study, based on direct-contact ultrasonic drying, provides basic data toward fundamental understanding of the application of ultrasound mechanism to drying of paper samples. Furthermore, the data provided in this paper will pave the way for validation of fundamentally developed models. For instance, the ultrasound pressure wave could be incorporated in the theoretical model by Noori et al..[21]

2. Materials and experimental method

Figure 1a illustrates the experimental setup for direct-contact ultrasonic drying. The major components in the experimental setup include: a power amplifier (AG 1014, T&C power), an ultrasound transducer (SMIST25F16RR112), a microbalance (Sartorius BCE6200, 0.001 g accuracy), and a FLIR infrared camera.

The results of ultrasonic drying were compared to those dried by direct-contact with a hot plate (Corning PC-420D). In this case, the samples were simply placed on the top of hot plate maintained at 80 °C.

In preparation of the hand-sheet samples, the procedure of TAPPI T205 standard was followed to get 150% dry-basis moisture content. For the samples with 100% dry-basis moisture content, the samples were dried at ambient until the desired initial moisture content was reached.

Four different pulps were used in the experiments: unrefined and refined softwood and hardwood. The pulps were Northern Bleached Hardwood Kraft (NBHK) and Northern Bleached Softwood Kraft (NBSK). The refining was done at the mill using the Beloit Double Disk refiner. The pulps had initial consistency of 4%. The pulp consistency is defined as the percentage by weight of ovendry fibers in a stock suspension (slurry). By adding water, the desired initial weight is obtained.

The diameter of the hand-sheet samples was 19.8 mm to precisely match the transducer's surface size. The mean thickness (t) of the hand-sheets was measured using a digital thickness gauge (accuracy 0.002 mm).

Figure 1b shows the piezoelectric transducer used in the experiments. This was a mist generator transducer with the resonant frequency of 1.7 MHz and its surface area was 314 mm^2. Since the sample needs to be in direct-contact with the transducer, the sample size is the same as the transducer (Figure 1c).

The changes in moisture content was measured by intermittent measurements of the sample's weight at 10 sec intervals. The dry-basis moisture content (DBMC) of the samples was calculated as:

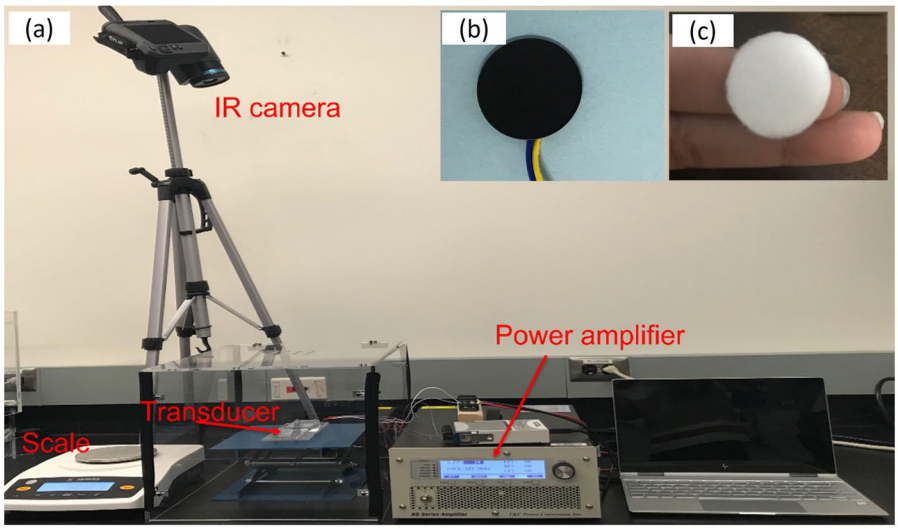

Figure 1. (a) The major components of the experimental setup, (b) ultrasonic transducer and (c) hand-sheet.

Table 1. The experimental derived uncertainty.

Derived Quantity	Maximum Uncertainty
DBMC	± 8.15 %
Whiteness Index	± 0.25 %
Change in color	± 3.04 %
Energy efficiency	± 5.61 %

$$DBMC = \frac{Weight\ \ of\ \ water}{Weight\ \ of\ \ dry\ \ matter} = \frac{m_t - m_{bone-dry}}{m_{bone-dry}} \tag{1}$$

where m_t is the mass of the sample at time t and $m_{bone\text{-}dry}$ is the mass of the totally dried sample, determined by drying it in an oven until its moisture is fully removed.

The uncertainty analysis for the derived quantities is calculated according to Kline and McClintock[22] and are given in Table 1.

The standard deviation of the reported experimental results for DBMC is 3.8, determined based on repeating each corresponding experiment five times.

Color analysis is done using colorimeter ColorFlex EZ. This device measures the color based on CIELAB color system ($\boldsymbol{L^*a^*b}$). The results of colorimeter measurements are used to calculate the change in color index (ΔE) and whiteness index (WI) for hand-sheets dried by ultrasound mechanism.

$$\Delta E = \sqrt{(L_2^* - L_1^*)^2 + (a_2^* - a_1^*)^2 + (b_2^* - b_1^*)^2} \tag{2}$$

$$WI = 100 - \sqrt{(100 - L^*)^2 + (a^{*2} + b^{*2})} \tag{3}$$

The 2 D porosity of the samples are estimated from microscopic images taken with Keyence VHX-7000 4k digital microscope. Thresholding is applied to the microscopic images to measure the pore volume percentage of the hand-sheets in 2 D using ImageJ software.[23] Non-contact profilometry measurements are performed using ZYGO 3 D profilometer. In addition, Multitest-dV Mecmesin device is used for measuring the tensile strength of the hand-sheets. The samples are chosen as rectangular shapes with about 19.8 mm in length and 5 mm in width. The length between the grips is fixed at 11 mm for all the tests conducted and therefore 9 mm of the length is in the grips' region.

3. Design of experiments

Factorial design is a systematic method for designing the experiments to determine the relationship between the factors in an experiment and the response value (outcome). In addition to the effect of individual factors, it also helps to understand the interactive effects of different factors in analyzing the results.[24] In this study, 2^3 factorial design was applied by considering three main factors: the initial moisture content, final thickness, and the refining condition of the pulp. Each factor has two levels in this design and the replicate number is 5. Minitab software was used for statistically analyzing the experimental results by applying analysis of variance (ANOVA). In the analysis, p-values less than 0.05 were considered statistically significant. The relationship between the response value of the experiments (i.e., the total time of drying) and the factors is investigated using a linear regression analysis as follows:

$$\begin{aligned} Y &= f(x) \\ &= \beta_0 + \sum_{i=1}^{k} \beta_i X_i + \sum_{i=1}^{k} \sum_{j=1}^{k} \beta_{ij} X_i X_j \\ &\quad + \beta_{123} X_1 X_2 X_3 + \beta_{cp} * CP \end{aligned} \tag{4}$$

Table 2. Upper and lower levels of factors for 2^3 factorial design of experiments for both hardwood (H) and softwood (S). R defines refined and unR defines unrefined.

	Factors		
Experiment Number	Refining Condition	Initial Moisture Content – DBMC (%)	Thickness (mm)
H or S-unR-100-0.3	Unrefined	100	0.3
H or S-unR-150-0.3	Unrefined	150	0.3
H or S-unR-100-0.6	Unrefined	100	0.6
H or S-unR-150-0.6	Unrefined	150	0.6
H or S-R-100-0.3	Refined	100	0.3
H or S-R-150-0.3	Refined	150	0.3
H or S-R-100-0.6	Refined	100	0.6
H or S-R-150-0.6	Refined	150	0.6
H or S-Center Point	50% Unrefined & 50% Refined	125	0.45

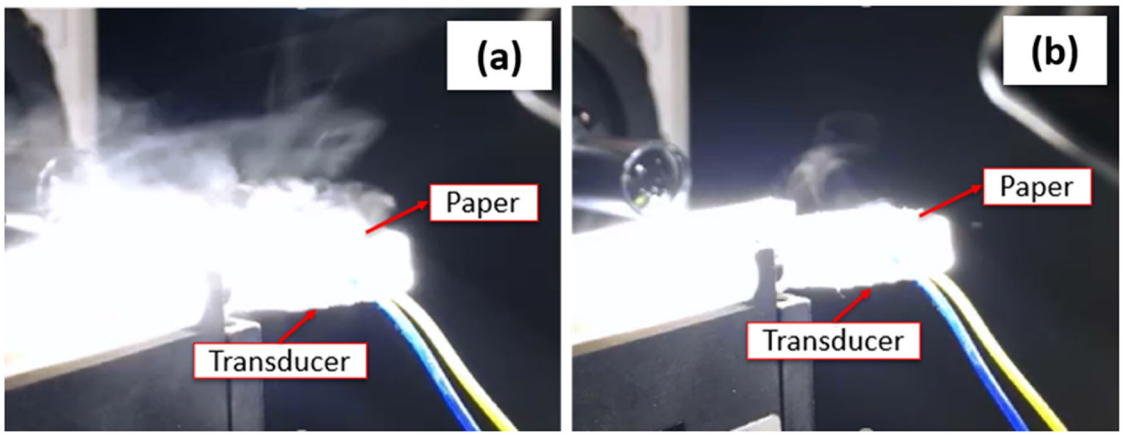

Figure 2. Comparing the ultrasonic atomization for (a) an over-saturated unrefined softwood hand-sheet with (b) an unrefined softwood hand-sheet with 150% DBMC.

where Y is the predicted response as a function of the factors; k is the number of factors, and X_i $(i = 1, 2, 3)$ are the controlling factors. β_0 is the constant coefficient, β_{ij} are the coefficients for the interactive effects of the factors and β_{123} captures the interactive effect of all the three factors. CP is the center point of the cube in 2^3 factorial design and β_{cp} is the coefficient for the center point.

Table 2 shows the nine designed experiments along with the upper and lower levels for each factor. In this table, the first 8 experiments are the corners of the cube and the nineth experiment is center point of the cube. Abbreviations are employed to define each of the experiments and are used in the remaining of the paper.

4. Results and discussion

4.1. Illustration of ultrasonic drying

As it was mentioned in the introduction, the mechanism of ultrasonic drying is atomization due to the mechanical vibrations. Figure 2 shows the atomization for two hand-sheet samples with two different moisture contents. Figure 2a shows the atomization for an over-saturated unrefined softwood hand-sheet and Figure 2b shows the atomization for the same unrefined softwood hand-sheet with moisture content 150% DBMC. For the over-saturated hand-sheet the amount of moisture that is removed by atomization is much higher than the moisture that is removed from the sample with 150% DBMC moisture content. Therefore, ultrasonic atomization rate is higher at higher moisture contents. With the overly saturated samples, the excess moisture resides on the sample surface, thus readily removeable by the ultrasonic mechanism.

Looking at the IR camera images of the unrefined hardwood hand-sheet (150% initial DBMC) placed on the surface of the transducer at selected times (Figure 3) implies that the temperature increases steadily from the center of the transducer toward the outside, which confirms that the center oscillates the most. A similar behavior was also observed in Ref.[10] in ultrasonic drying of a fabric sample. Temperature measurements during the ultrasonic drying experiments revealed that the temperature of the surface of the sample increases up to about 80 °C before complete drying. Hence, it is concluded that the dominant mechanism for direct-contact

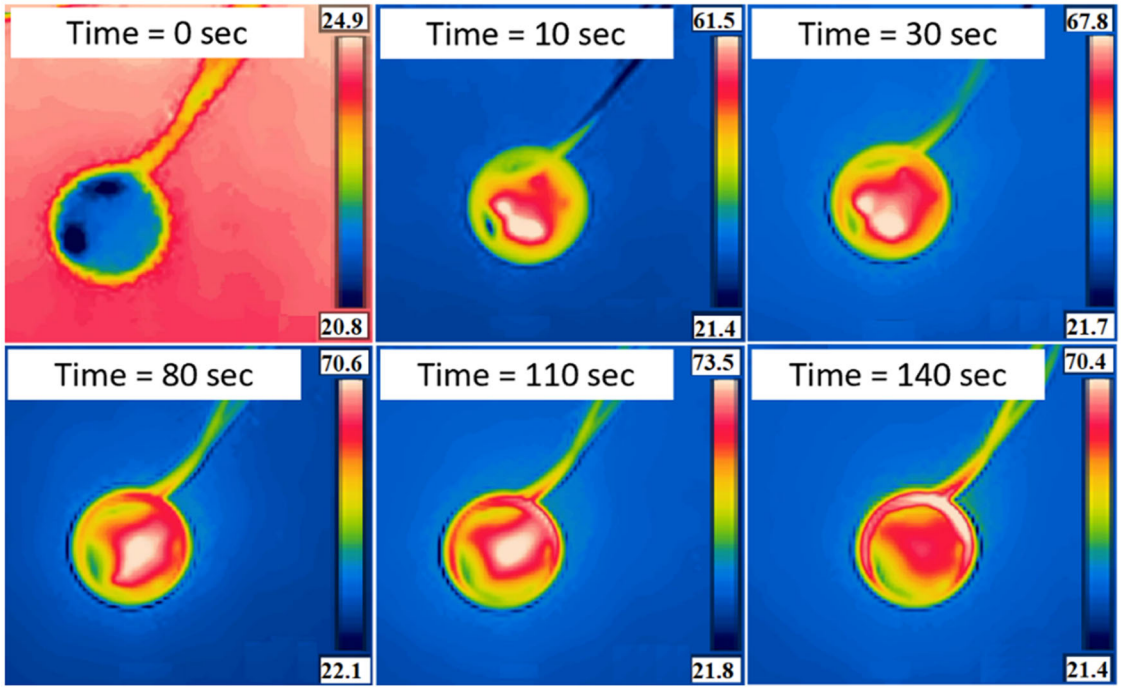

Figure 3. Selected IR image sequences at different times of ultrasonic drying for unrefined hardwood hand-sheet (150% initial DBMC) placed on top of the transducer. The temperatures are in °C.

ultrasonic drying initially is atomization but at the final stages of drying, heating is also important. In addition, as the hand-sheet dries and moisture content decreases, due to the bulging effect, the temperature of the hand-sheet decreases.

4.2. Comparing ultrasonic drying with conductive heat drying

To have a better illustration of the effect of ultrasound mechanism on drying, thermal drying of hand-sheets is conducted at temperature equal to 80 °C to extract the sole impact of ultrasound.

Figure 4 compares the drying curves for an ultrasonically dried hand-sheet with a hand-sheet dried using conductive heating at 80 °C. This figure shows that in the presence of ultrasound mechanism, the drying time decreases by almost 30% and hence, ultrasonic drying is faster than conductive drying under the operating conditions considered here. This finding confirms the favorable effect of atomization in ultrasonic drying. Many studies (e.g., 15 and 17) have shown that the ultrasonic atomization enhances the heat and mass transfer coefficients, supporting the results reported in this study.

4.3. Analysis of the factorial design of experiments

Figure 5 is representing the ultrasonic drying curves for hardwood and softwood, respectively. The plots are at different combinations of initial moisture content, thickness, and refining condition of the pulps.

Ultrasonic drying takes place in two phases: a relatively constant-rate drying period followed by a falling-rate drying period. The constant drying rate period corresponds to the removing of free water within the pores of paper, while the falling drying rate period is governed by the associated (bound) water trapped inside the fibers. This is typical regardless of drying mechanism.

Comparing the plots in Figure 5 implies that in general, unrefined samples dry faster than refined samples and the drying time for softwood is lower than for hardwood. In addition, increasing the thickness and the initial moisture content of the sample increase the drying time. The shortest and longest drying times correspond to S-unR-100-0.3 and H-R-150-0.6, respectively. These observations are potentially related to the sheet formation, impacting the pore structure. In general, hardwood has lower Canadian Standard Freeness (CSF) and higher Water Retention Value (WRV) compared to softwood, which makes it harder to dry. It is important to mention that for refined samples, these results may vary depending on the refining method. Furthermore, hardwood is denser than softwood and therefore its permeability is lower. This will be addressed in more detail in the next sections.

To analyze the results of the 2^3 factorial design of experiments, the response value is considered as the total time of drying which is discussed in the next section.

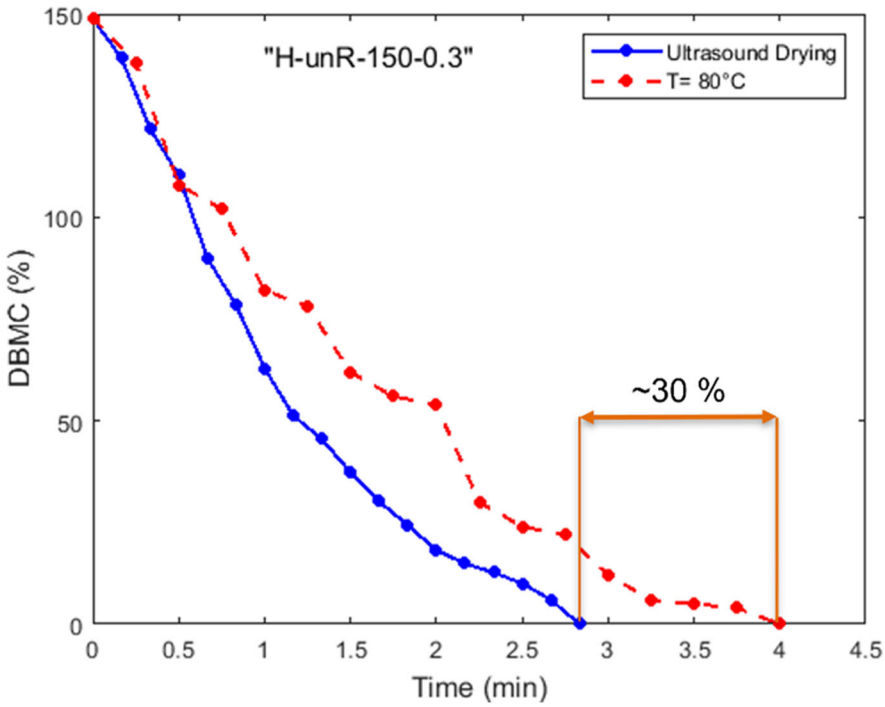

Figure 4. Comparing the drying curves for conductive heating with ultrasonic drying for an unrefined hardwood hand-sheet with 150% initial DBMC.

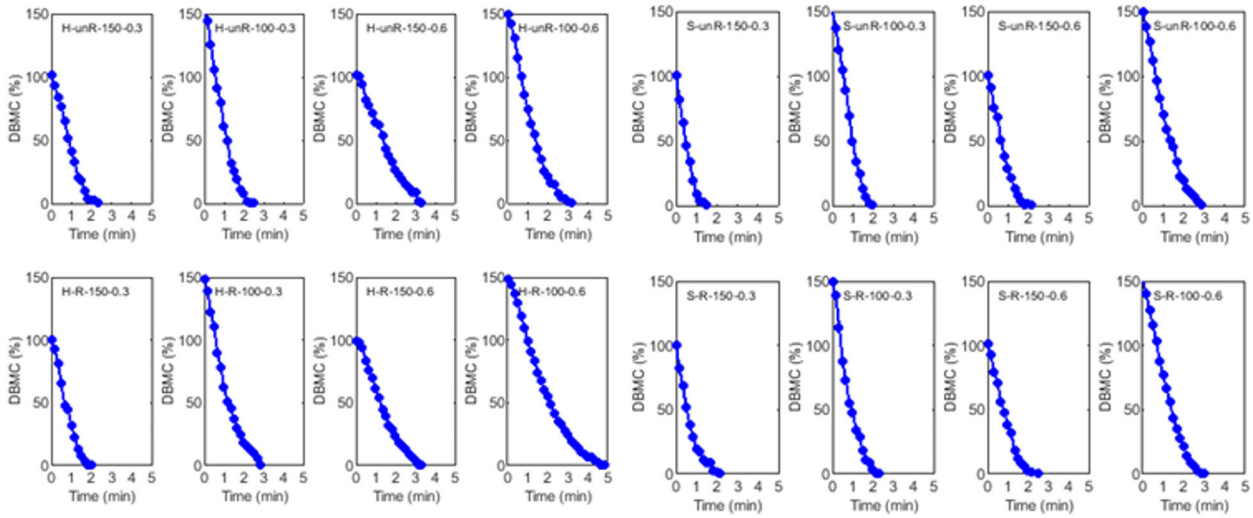

Figure 5. Ultrasonic drying curves for refined and unrefined hardwood and softwood samples.

4.4. Effect of controlling factors on total drying time

The Analysis of Variance (ANOVA) is done for both hardwood and softwood samples and each experiment is repeated 5 times. Figure 6 shows the Pareto charts of the standardized effects, which determines the magnitude and the importance of the effects, both for the main factors and their interactive effects. The reference line, the red line on the charts, depends on the significance level, which is defined as 0.05 in this study and the bars that cross this reference line are statistically significant. Figure 6 shows that for both hardwood and softwood, of the parameters explored, thickness has the maximum effect on ultrasonic drying time followed by initial DBMC and refining condition of the pulp. The interactive effects of the parameters are less important for predicting the ultrasonic drying time. The results of linear regression analysis for total time of ultrasonic drying are reported in Table 3. The coefficients of determination, R^2, are 99.43% and 95.28%, meaning that the model could

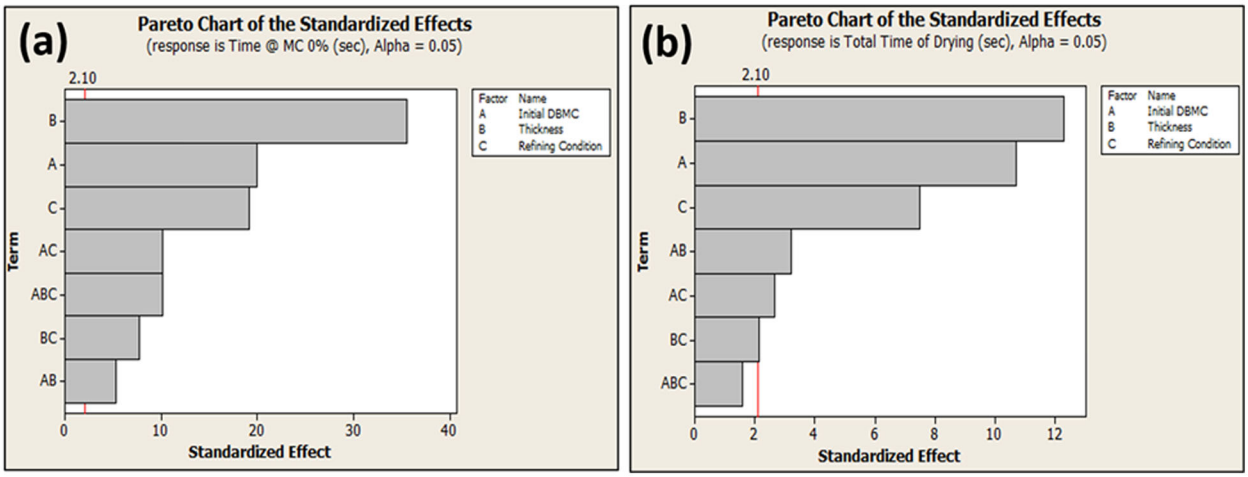

Figure 6. Pareto charts of the standardized effects from ANOVA analysis for total time of ultrasonic drying: (a) hardwood and (b) softwood.

Table 3. Coefficients for equation (4) calculated from linear regression analysis.

		β_0	β_1	β_2	β_3	β_{12}	β_{13}	β_{23}	β_{123}	β_{CP}	R^2 (%)
Hardwood	Drying time (sec)	50	0.167	61.111	100	1.444	−0.833	−294.444	−2.778	−11.25	99.43
	Whiteness index	74.889	−0.014	−4.13	−1.809	0.086	0.012	4.796	−0.018	0	97.4
Softwood	Drying time (sec)	68.333	0.067	−38.889	5	1.333	0.133	61.111	−0.667	0.833	95.28
	Whiteness index	55.307	0.101	42.156	−0.218	−0.273	0.004	0.732	−0.008	0	96.2

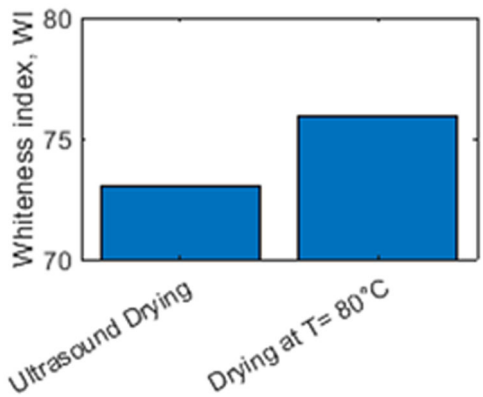

Figure 7. Comparison of whiteness index for ultrasonic drying with heat conductive drying at 80 °C for H-R-150-0.3.

account for 99.43% and 95.28% variability in data, respectively for hardwood and softwood. Based on the ANOVA analysis, the models show a significant effect of the considered factors on drying time ($p < 0.01$). These data imply that the predicted correlations by linear regression analysis are adequate in describing the drying time.

It should be noted that there is a lack of detailed fundamental work on ultrasonic dehydration in the literature, and therefore no in-depth understanding of the phenomena in moist porous material. Recently, the author in[25] has explored the ultrasonic atomization phenomena in microscale and has investigated the impacts of non-dimensional parameters on the process, including Reynolds number, Webber number, Strouhal number, and Froud number.

The quality of the product is a very important factor in determining the applicability of any drying technology. In the next sections, the measurements related to color, microstructure, surface roughness, and the tensile strength of the hand-sheets dried using ultrasound mechanism are provided.

4.5. Colorimeter measurements

Figure 7 compares the whiteness index for an ultrasonically dried hand-sheet (H-R-150-0.3) with a sample dried using conductive heating at 80 °C. This figure shows that direct-contact ultrasonic drying slightly improves the whiteness index and therefore the product quality.

The results of colorimeter measurements for the change in color index (ΔE) and whiteness index (WI) for ultrasonically dried hand-sheets are shown in Figure 8.

Change in color after drying is between 1 to 6 and the whiteness index is higher for softwood compared to hardwood samples (Figure 8).

The results represent that overall the whiteness index for unrefined samples are higher than refined samples. In addition, increasing the thickness and increasing the initial moisture content, increase WI. The enhancement of lightness and whiteness index with increasing the thickness is an implication of increasing the porosity of the samples with increasing

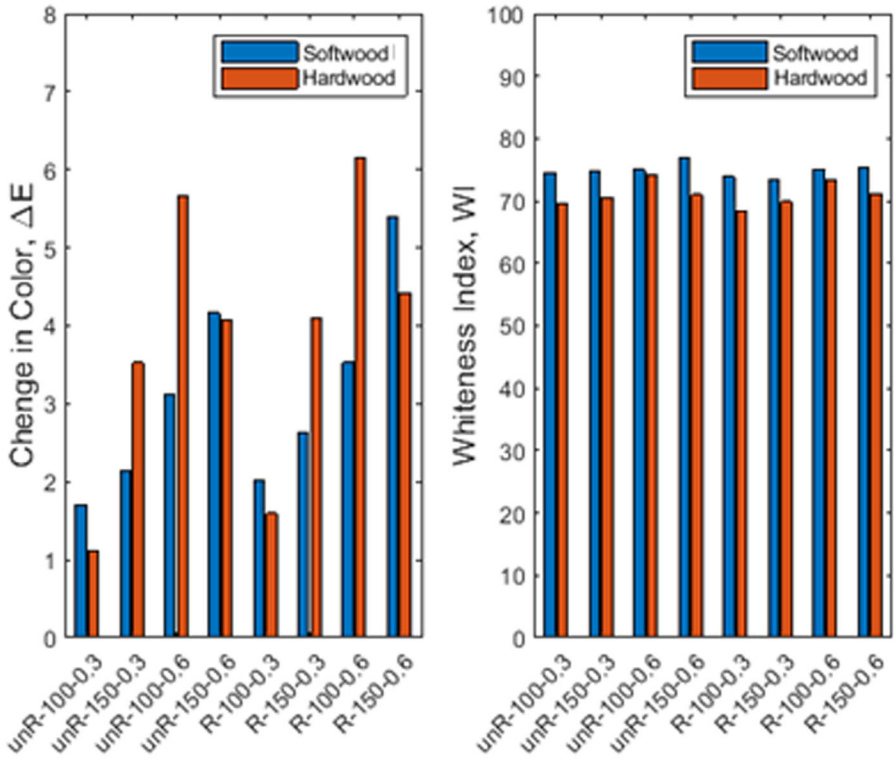

Figure 8. Change in color and whiteness index of ultrasonically dried hand-sheets.

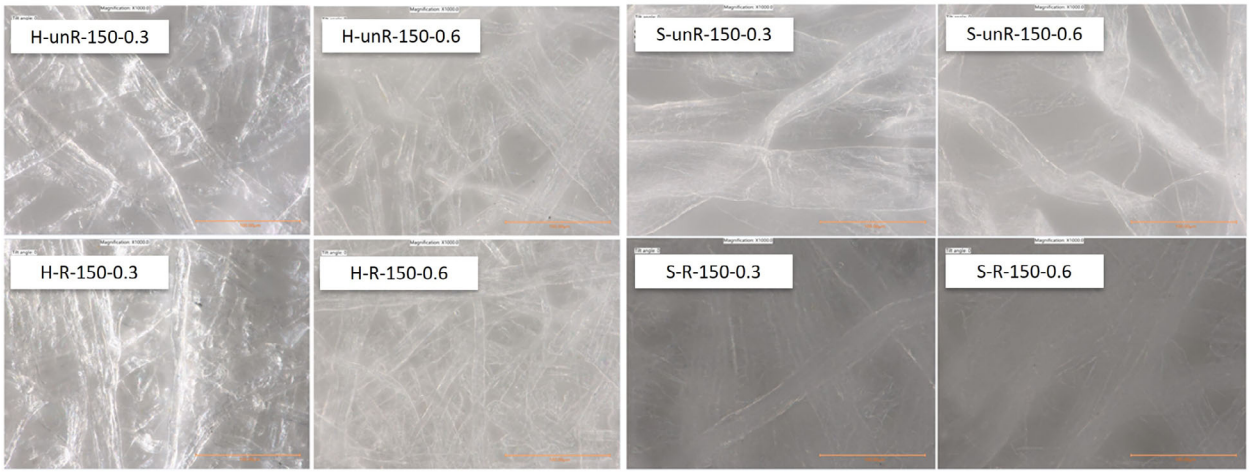

Figure 9. Optical microscopic images for hardwood and softwood samples dried with ultrasound mechanism. The initial DBMC for all the samples is 150%. Magnification is 1000X.

the thickness. More details will be addressed in the next section.

ANOVA analysis is done for WI and the results show that thickness has the maximum effect on WI of the hand-sheets dried with ultrasound mechanism. The results of linear regression analysis are reported in Table 3.

4.6. Microscopic measurements

Paper is a porous medium and one of the important parameters in determining its properties is porosity (ε). Figure 9 shows the pore distribution in the optical microscopic images for hardwood and softwood hand-sheets. It should be noted that the initial DBMC for all these samples is 150%.

Comparing the microscopic images for hardwood and softwood reveals the differences in the fiber sizes and pore sizes in different samples. Unrefined samples have larger pores compared to refined samples, while refined fibers are more uniform compared to unrefined fibers. Additionally, the fibers are coarser and longer in unrefined samples. Softwood samples have

coarser fibers compared to hardwood samples. Using ImageJ software,[23] thresholding is applied to these microscopic images to measure the pore volume percentage of the hand-sheets in 2 D. Figure 10 summarizes the results of these 2 D measurements. This figure shows higher pore volume for unrefined samples compared to refined samples. 2 D pore volume for softwood samples is higher than hardwood samples. Increasing the thickness, slightly increases the pore volume. These findings are evident that unrefined samples dry faster than refined samples and the drying rate for softwood is higher than that for hardwood.

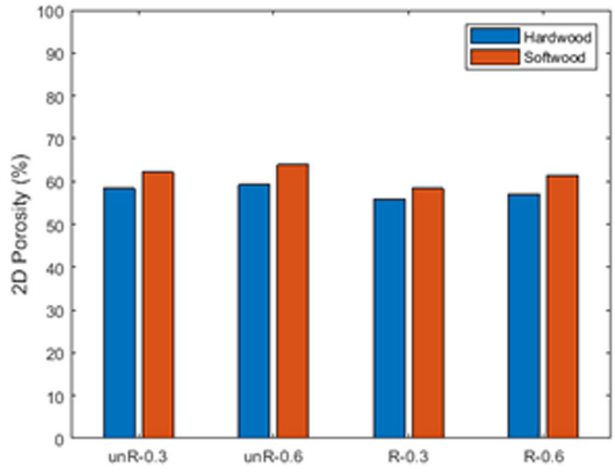

Figure 10. 2 D pore volume measurements using thresholding of the microscopic images of samples dried with ultrasound mechanism. The initial DBMC for all the samples is 150%.

4.7. Profilometry measurements

Color view of the surface profiles for hardwood and softwood samples are shown in Figure 11. It should be noted that the initial DBMC for all these samples is 150%.

The surface roughness depends on the species and texture uniformity. In this study, TAPPI T205 standard is used for preparing the samples, however the bulging effect during the experiments might have influenced the smoothness of the surface and its uniformity.

Figure 12 shows the results of profilometry measurements. The maximum standard deviation is 0.05. *Sa* is the average roughness, *Sq* is the root mean square roughness evaluated over the complete 3 D surface. *Sz* is the maximum height of the areal surface, which is the peak to valley height. Figure 12 shows that refined samples have lower roughness compared to unrefined samples. Overall, the roughness index for softwood samples is higher than hardwood samples. Hardwood samples are more uniform, and they are more suitable for producing smoother surfaces. Qualitatively, the important point here is that ultrasonic drying does not change the behavior of softwood and hardwood after drying.

4.8. Tensile strength measurements

Tensile strength plays a significant role in various applications of paper products.

Figure 13 compares the tensile strength for H-R-150-0.3 dried using ultrasound mechanism and using conductive heating at 80 °C. The results show that

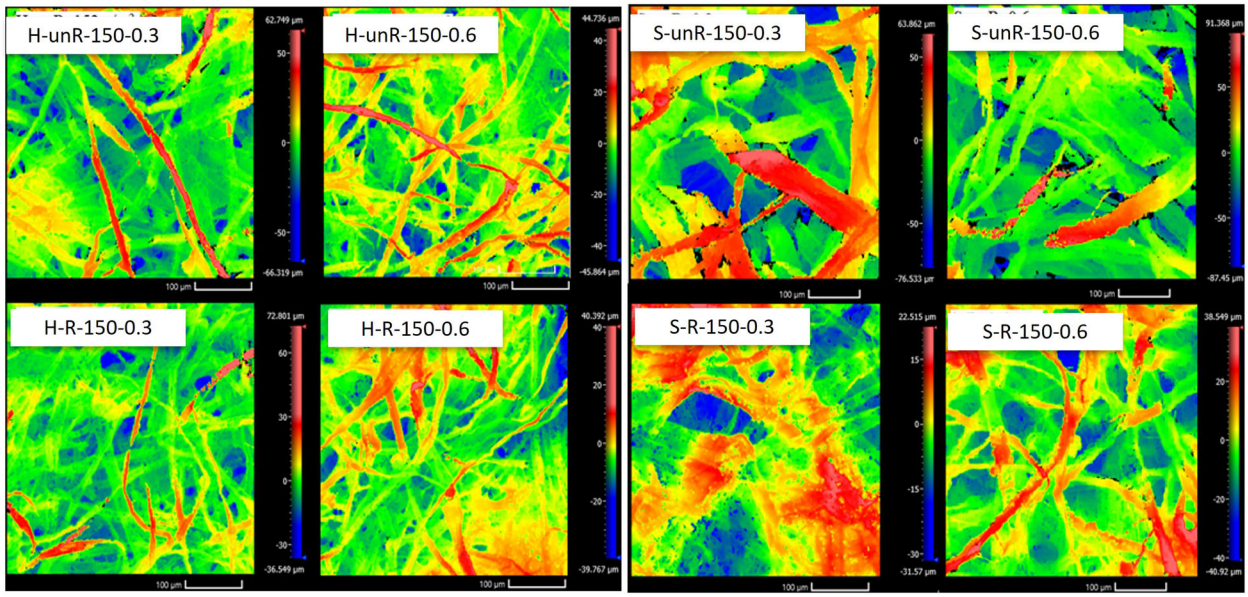

Figure 11. Color view of roughness measurements for hardwood and softwood samples. It should be noted that the initial DBMC for all the samples is 150%.

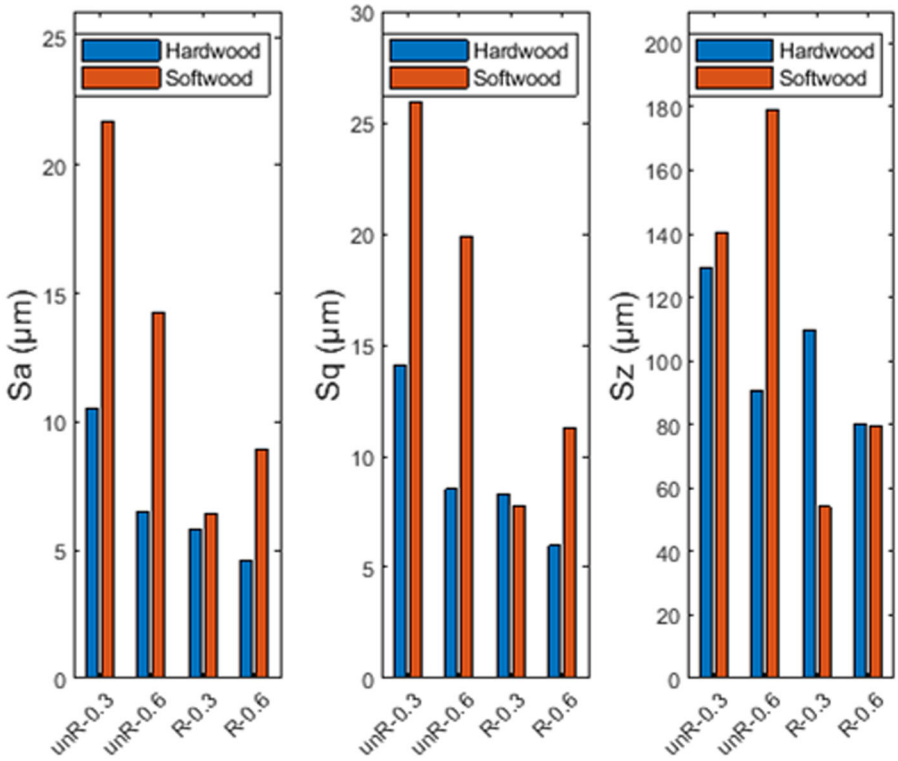

Figure 12. Surface roughness measurements for samples dried with ultrasound mechanism. The initial DBMC for all the samples is 150%.

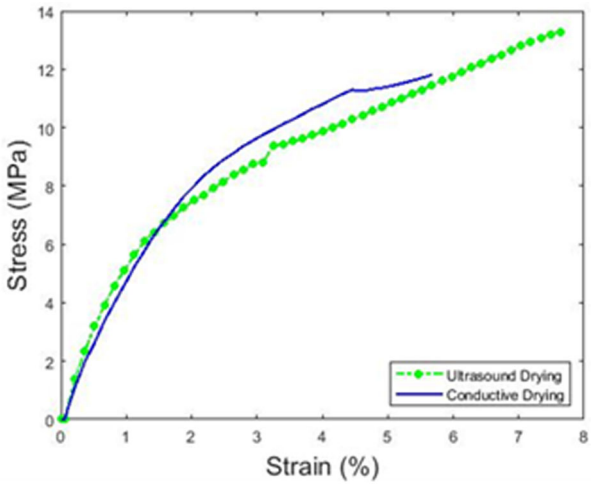

Figure 13. Comparing stress-strain curves for H-R-150-0.3 with ultrasonic drying and with conductive heat drying at 80 °C.

ultrasonic drying does not seem to decrease the tensile strength.

The tensile strength measurements revealed that moisture content does not show much influence on the tensile strength of the dried samples within the range of the parameters considered in this study. The stress-strain curves for the samples at 100% DBMC and for the center points are illustrated in Figure 14 and Table 4 summarizes the results. In general, the refined pulps have a higher ultimate tensile strength (UTS) compared to that of unrefined pulps. According to Motamedian et al.,[26] refining is a common procedure in paper making industry to improve the mechanical properties of the final product. In addition, the tensile strength is affected by the sample basis weight and thickness. The hand-sheet with a higher thickness has a lower strength because of the stress gradients in the thickness direction. Hagglund et al.[27] proposed a linear elastic 2 D finite element analysis to model the stress field under the jaws. The model proposes that the clamping condition during the test results in higher stresses at the surface and lower stresses in the middle of the sheet. Batchelor et al.[28] showed that the level of stress concentration highly depends on the thickness and the grammage of the paper samples. As a result of the stress gradients in the thickness direction, increasing thickness and grammage reduces the strength of the sample. Furthermore, the tensile strength for the center points is between the tensile strengths for refined and unrefined samples.

4.9. Energy analysis

It is very important to apply sufficient electrical power to the transducer to induce atomization of water in the moist medium. For the transducer used in this

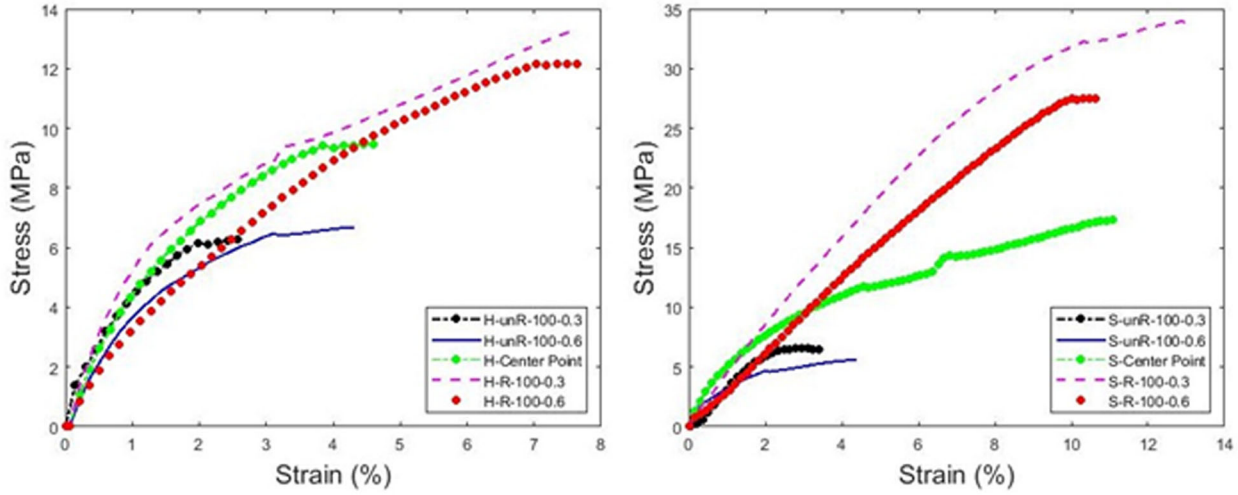

Figure 14. Stress-strain curves for different types of pulps with different thicknesses.

Table 4. Ultimate tensile strain and ultimate tensile stress for different samples.

Sample	Ultimate Tensile Strain (%)	Ultimate Tensile Strength (MPa)
H-unR-100-0.3	2.58	6.28
H-unR-100-0.6	4.31	6.67
H-Center Point	4.6	9.47
H-R-100-0.3	7.64	13.29
H-R-100-0.6	7.63	12.15
S-unR-100-0.3	4.4	5.57
S-unR-100-0.6	3.39	6.6
S-Center Point	11.07	17.29
S-R-100-0.3	13.05	33.93
S-R-100-0.6	10.61	27.49

study under the operating frequency of 1.7 MHz, 10 W power is applied to allow for the atomization to take place. As the sample dries, due to the changes in impedance, the load power to the transducer changes by drying time. The records show that the changes of load power, for the transducer used in this study, during all the experiment is almost the same and it is represented in Figure 15.

The following equation is defined to calculate the energy factor (EF), which is defined as the ratio of the thermal energy required for evaporation to the total load power (LP) applied to the transducer:

$$EF = \frac{(m_0 - m_t)h_{fg}}{\int_0^t LP(t)dt} \quad (5)$$

where m_0 and m_t are the initial and the instantaneous weight of the sample. h_{fg} is the latent heat of evaporation and it is assumed to be constant at 2500 kJ/kg. t is the time.

Figure 16 compares the energy factor for all the experiments conducted as a function of time. The

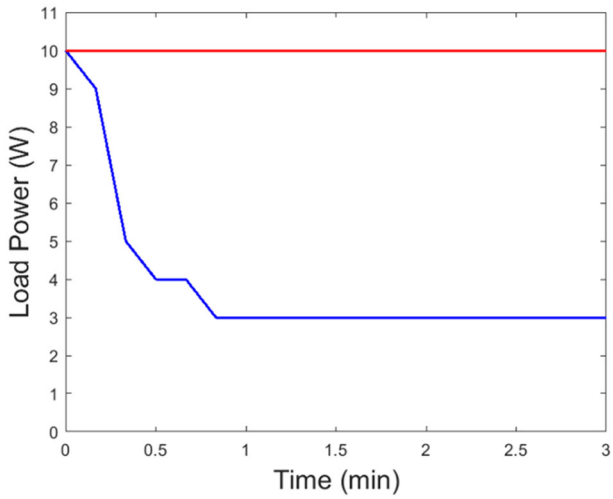

Figure 15. Changes in load power as a function of drying time. 10 W forward power is applied to the transducer (red line).

energy factor initially increases with the drying time mainly because of the increase in the direct contact ultrasound transducer surface temperature. However, after reaching its maximum, it decreases simply due to the drop in the available moisture to atomize especially on the sample surface exposed to the ambient air. The overall results confirm that, the unrefined samples have higher energy factors compared to refined samples. This finding agrees with the fact that unrefined samples dry faster than refined samples. Increasing the basis weight (thickness) of the samples increases the energy efficiency and partially it is related to the porosity of the sample as discussed in previous sections. In general, the results show that ultrasonic drying is less energy efficient compared to direct thermal drying for the operating conditions considered in this study. As it was illustrated in

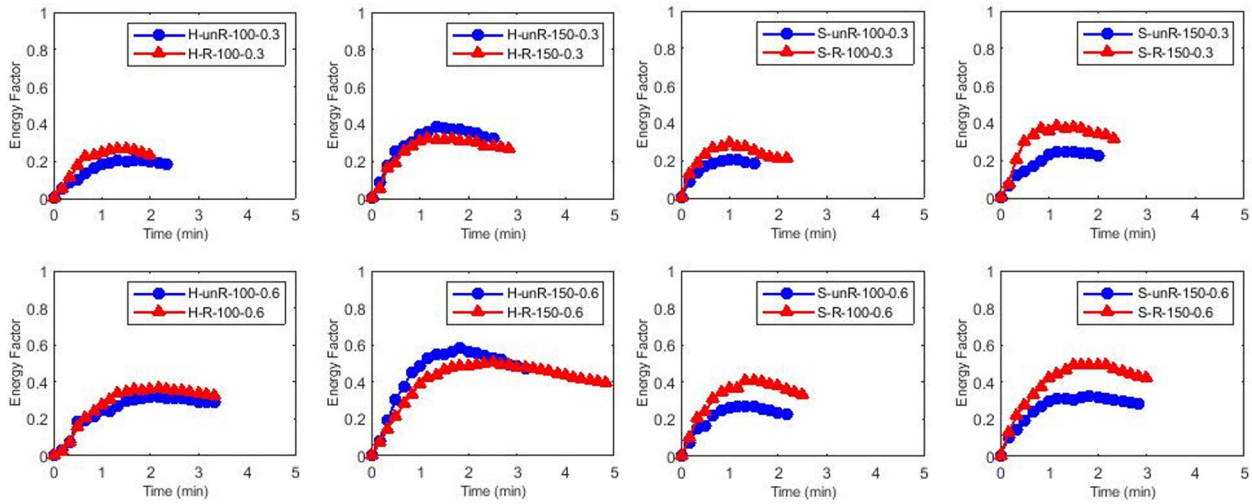

Figure 16. Comparing the energy factor for hardwood and softwood samples.

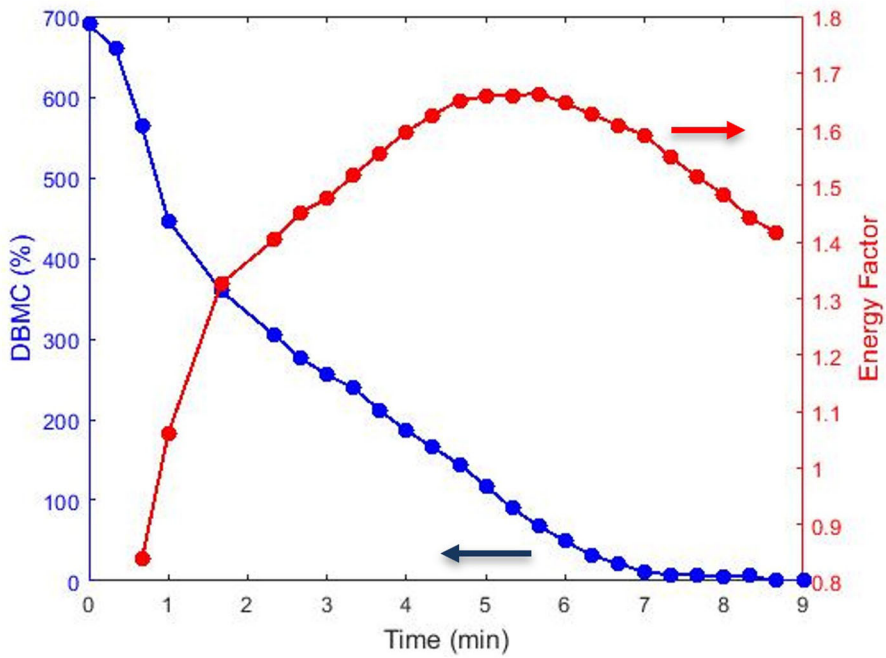

Figure 17. Illustration of the effect of high moisture content on DBMC and energy factor for H-R-700-0.3.

Section 4.1, ultrasonic drying has higher drying rates at higher moisture contents. This can be observed from the energy factor plots in Figure 16, which energy factor is higher at 150% DBMC compared to that of 100% DBMC. To confirm the effectiveness of ultrasonic drying at high moisture content levels, an additional test was conducted with a paper hand-sheet with initial DBMC of 700% (H-R-700-0.3). As shown in Figure 17, the ultrasound energy factor reaches to about 1.7, illustrating the increase in effectiveness of ultrasonic drying with the increase in moisture content.

5. Summary and conclusions

Hardwood and softwood hand-sheet samples are dried using direct-contact ultrasound mechanism. The results confirm that ultrasonic drying mechanism is more efficient at higher moisture content levels. IR camera images for the temperature on the surface of the transducer revealed that by applying ultrasound, first the temperature in the center increases and then by propagating the oscillations through the surface of the transducer, the temperature increases through the surface. Comparing the drying curve of ultrasound

mechanism with the drying curve from thermal drying at 80 °C showed a significant decrease in drying time. ANOVA is done for both hardwood and softwood. The independent factors in the analysis are including initial moisture content, thickness, and refining condition of the pulp and two high and low levels are considered for each factor. The results showed that for the total time of ultrasonic drying, the thickness has the maximum effect and after that initial moisture content is important. These findings for ultrasonic drying behavior of paper samples are related to the structural characteristics of the samples. Therefore, microstructure of the samples is investigated and the surface profilometers are measured. The results showed that softwood fibers are coarser than hardwood fibers. Therefore, the pores in softwood are larger and the porosity is higher compared to hardwood. In addition, unrefined samples have larger pores compared to refined samples and hence, unrefined dries faster. Therefore, as it is expected, the structure of the sample (refined, unrefined, or a mixture) has a significant impact on drying curve. The quality of the ultrasonically dried samples is measured using colorimeter analysis for whiteness index. Using regression analysis two equations for both hardwood and softwood are provided. These equations describe the total time of drying and whiteness index. To analyze the energy efficiency of the ultrasonically dried samples, energy factor (EF) is defined as the ratio of the energy required for evaporation to the energy that generates the ultrasonic vibrations. The higher energy factor means the process is more energy efficient. The results showed that the energy factor for direct-contact ultrasonic drying for the current setup is 0.2-0.6. This implies that better design of transducers is required to increase the efficiency of the process. Furthermore, increasing the initial moisture content to 700% results in higher energy efficiency for ultrasonic drying compared to thermal drying. The energy factor for unrefined samples is higher than refined samples, which agrees with the fact that unrefined samples dry faster than refined samples. The refined samples show higher tensile strength comped to that of unrefined samples. This study provides the foundation for the next studies of fundamental understanding of ultrasound mechanism for hand-sheet drying.

Disclosure statement

No potential conflict of interest was reported by the authors.

Funding

This study was supported by the Center for Advanced Research in Drying (CARD), a US National Science Foundation Industry/University Cooperative Research Center. CARD is located at Worcester Polytechnic Institute and University of Illinois at Urbana-Champaign (co-site). The authors acknowledge Mr. David Turpin technical contribution to this study. The pulps used in this study were provided by Domtar and the authors appreciate this.

References

[1] Mujumdar, A. S. *Book Review: Handbook of Industrial Drying: A Review of;* CRC Press: Boca Raton, FL, **2007**.

[2] Li, J.; Kong, L.; Liu, H. Dryer Section Energy System Measurement and Energy-Saving Potential Analysis for a Paper Machine. *Meas. Control* **2012**, *45*, 239–243. DOI: 10.1177/002029401204500803.

[3] Hnin, K. K.; Zhang, M.; Mujumdar, A. S.; Zhu, Y. Emerging Food Drying Technologies with Energy Saving Characteristics: A Review. *Dry. Technol.* **2019**, *37*, 1465–1480. DOI: 10.1080/07373937.2018.1510417.

[4] Gallego-Juarez, J. A.; Rodriguez-Corral, G.; Galvez Moraleda, J. C.; Yang, T. S. A New High-Intensity Ultrasonic Technology for Food Dehydration. *Dry. Technol.* **1999**, *17*, 597–608. DOI: 10.1080/07373939908917555.

[5] Mujumdar, A. S. *Drying Technology in Agriculture and Food Science;* Science Publishers: Enfield, **2000**.

[6] Khaire, R. A.; Gogate, P. R. Novel Approaches Based on Ultrasound for Spray Drying of Food and Bioactive Compounds. *Dry. Technol.* **2021**, *39*, 1832–1853. DOI: 10.1080/07373937.2020.1804926.

[7] Raso, J.; Manas, P.; Pagan, R.; Sala, F. J. Influence of Different Factors on the Output Power Transferred into Medium by Ultrasound. *Ultrason. Sonochem.* **1999**, *5*, 157–162. DOI: 10.1016/S1350-4177(98)00042-X.

[8] Mulet, A.; Carcel, J. A.; Sanjua, N.; Bon, J. New Food Drying Technologies-Use of Ultrasound. *Food Sci. Technol. Int.* **2003**, *9*, 215–221. DOI: 10.1177/1082013203034641.

[9] Chen, Y.; Li, M.; Shashikala Kumari Dharmasiri, T.; Song, X.; Liu, F.; Wang, X. Novel Ultrasonic-Assisted Vacuum Drying Technique for Dehydrating Garlic Slices and Predicting the Quality Properties by Low Field Nuclear Magnetic Resonance. *Food Chem.* **2020**, *306*, 125625.

[10] Peng, C.; Ravi, S.; Patel, V. K.; Momen, A. M.; Moghaddam, S. Physics of Direct-Contact Ultrasonic Cloth Drying Process. *Energy* **2017**, *125*, 498–508.

[11] Li, P.; Chen, Z. Experiment Study on Porous Fiber Drying Enhancement with Application of Power Ultrasound. *Appl. Acoust.* **2017**, *127*, 169–174. DOI: 10.1016/j.apacoust.2017.06.003.

[12] Peng, C.; Moghaddam, S. Experimental Evaluation and Kinetic Analysis of Direct-Contact Ultrasonic Fabric Drying Process. *J. Therm. Sci. Eng. Appl.* **2021**, *13*, 1–11.

[13] Zhang, Y.; Abatzoglou, N. Fundamentals, Applications and Potentials of Ultrasound-Assisted Drying. *Chem. Eng. Res. Des.* **2020**, *154*, 21–46. DOI: 10.1016/j.cherd.2019.11.025.

[14] Mujumdar, A. S. Research and Development in Drying: Recent Trends and Future Prospects. *Dry. Technol.* **2004**, *22*, 1–26. DOI: 10.1081/DRT-120028201.

[15] García-Pérez, J. V.; Cárcel, J. A.; Benedito, J.; Mulet, A. Power Ultrasound Mass Transfer Enhancement in Food Drying. *Food Bioprod. Process.* **2007**, *85*, 247–254. DOI: 10.1205/fbp07010.

[16] Andrés, R. R.; Riera, E.; Gallego-Juarez, J. A.; Mulet, A.; Garcia-Perez, J. V.; Carcel,.; J.; A. Airborne Power Ultrasound for Drying Process Intensification at Low Temperatures: Use of a Stepped-Grooved Plate Transducer. *Dry. Technol.* **2021**, *39*, 245–258. DOI: 10.1080/07373937.2019.1677704.

[17] Legay, M.; Gondrexon, N.; Le Person, S.; Boldo, P.; Bontemps, A. Enhancement of Heat Transfer by Ultrasound: Review and Recent Advances. *Int. J. Chem. Eng.* **2011**, *2011*, 1–17. DOI: 10.1155/2011/670108.

[18] Rahimi, M.; Abolhasani, M.; Azimi, N. High Frequency Ultrasound Penetration through Concentric Tubes: Illustrating Cooling Effects and Cavitation Intensity. *Heat Mass Transfer* **2015**, *51*, 587–599. DOI: 10.1007/s00231-014-1435-9.

[19] Momen, A. M.; Kokou, E.; Bansal, P.; Gluesenkamp, K. R.; Abdelaziz, O. **2015** Preliminary Investigation of Novel Direct Contact Ultrasonic Fabric Drying. In *ASME 2015 International Mechanical Engineering Congress and Exposition*. American Society of Mechanical Engineers Digital Collection. DOI: 10.1115/IMECE2015-50479.

[20] Yang, G.; Zhu, J. J. *Handbook of Ultrasonics and Sonochemistry*; Springer: Singapore, **2016**.

[21] Noori, Z.; Yagoobi, J. S.; Tilley, B. S. Fundamental Understanding of Removal of Liquid Thin Film Trapped between Fibers in the Paper Drying Process: A Microscopic Approach. *Tappi J.* **2020**, *19*, 249–258. DOI: 10.32964/TJ19.5.249.

[22] Kline, S. J.; McClintock, F. A. Describing Uncertainties in Single-Sample Experiemts. *ASME Mech. Eng.* **1952**, *75*, 3–8.

[23] Abramoff, M. D.; Magalhaes, P. J.; Ram, S. J. Image Processing with ImageJ. *Biophotonics Int.* **2004**, *11*, 36–42.

[24] Montgomery, D. C. *Design and Analysis of Experiments;* John Wiley & Sons: New Jersey, **2017**.

[25] Noori, O.; Z. Fundamental Understanding of Removal of Water Trapped inside and outside Paper Fibers and Ultrasonic Drying of Paper Hand-Sheets. PhD Dissertation, Worcester Polytechnic Institute, Worcester, MA, **2022**.

[26] Motamedian, H. R.; Halilovic, A. E.; Kulachenko, A. Mechanisms of Strength and Stiffness Improvement of Paper after PFI Refining with a Focus on the Effect of Fines. *Cellulose* **2019**, *26*, 4099–4124. DOI: 10.1007/s10570-019-02349-5.

[27] Hägglund, R.; Gradin, P.; Tarakameh, D. Some Aspects on the Zero-Span Tensile Test. *Exp. Mech.* **2004**, *44*, 365–374. DOI: 10.1007/BF02428089.

[28] Batchelor, W. J.; Westerlind, B. S.; Hagglund, R.; Gradin, P. Effect of Test Conditions on Measured Loads and Displacements in Zero-Span Testing. *Tappi J.* **2006**, *5*, 3–8.